ELSEVIER

Contents lists available at ScienceDirect

International Journal of Mass Spectrometry

journal homepage: www.elsevier.com/locate/ijms



A perspective on the theoretical and numerical aspects of Ion Mobility Spectrometry



Carlos Larriba-Andaluz

Department of Mechanical and Energy Engineering, IUPUI, Indianapolis, 46202, USA

ARTICLE INFO

Article history:
Received 18 August 2021
Received in revised form
27 September 2021
Accepted 29 September 2021
Available online 2 October 2021

Keywords:
Ion mobility
Collision cross section
Mass spectrometry
Drift velocity
Monte Carlo

ABSTRACT

Ion Mobility Spectrometry (IMS) has become a ubiquitous analytical technique, in particular when used as an orthogonal technique to Mass Spectrometry (MS). As separations of ions in the gas phase become more precise, the need to provide a suitable theory that explains the observed differences is apparent. While the theory exists, much of it is obscured due to the difficulty of the equations and the approximations to the solution. This work explores some of the more useful theoretical approaches to IMS while making use of a full Monte Carlo simulations algorithm to provide some pedagogical examples that characterize the reasons behind the different theoretical approaches, and whether they need to be used for a particular calculation. To improve the existing theory, reliable empirical data is required. For such reason, an appropriate labeling system for mobility is proposed here requiring that at least the temperature, gas, electric field, and instrument employed are provided and which is an extension of the previous protocol.

© 2021 Published by Elsevier B.V.

1. Introduction

Ion Mobility Spectrometry (IMS) has undoubtedly reached maturity in the last decade while becoming one of the most employed techniques in hyphenation with Mass Spectrometry (MS) [1]. As more analytical chemists become aware of the benefits of Ion Mobility and as IMS systems become more sensitive and accurate, two distinct issues arise. The first one deals with the fact that new users are inexperienced with the theoretical aspects of the technique and therefore need to be instructed on what is possible and what is not, regarding existing theory. The second deals with the necessity to improve the common theory approximations that are unable to explain some of the behaviors that start to appear with higher resolution systems. These two points, while not mutually exclusive, have the additional problem that regular users normally do not have the time to improve the theory over what is readily available and that theoreticians are sometimes too far removed from existing experimental trends focusing on more subtle theoretical aspects that cannot be proven empirically with the existing knowledge. This also suggests that suitable protocols must be in place in order to describe measurements in a way that they can be replicated and can serve as empirical data that can be employed to further improve the theory.

The idea behind this work is to describe possible ways to understand and calculate mobility, both from a physical and an analytical perspective. The physical notion of how the ion behaves naturally in the presence of a gas is generally quite disregarded in ion mobility theory in favor of more compact theoretical expressions that many times obscure their physical meaning, with the user having trouble knowing whether the expression is applicable to their own calculation. A mixture of an introduction to kinetic theory and Monte Carlo simulations are combined to explain the reasoning behind many of the existing equations and how, if possible, to improve them. This is done from the author's perspective so not all issues regarding ion mobility might be addressed. The work starts with the standard formulation employed, followed by careful explanations of where the theory might fail and where/how to improve the calculation. Some more laborious theoretical aspects are left out of the manuscript but referenced so that the appropriate reader may access it where necessary. Finally, a description of how mobility should be labeled in IMS empirical data is brought forth and supported by the explanations in the manuscript. There are plenty of thorough references on the topic that the reader should consult as well [1-10].

* Corresponding author E-mail address: clarriba@iupui.edu.

2. Basic theory regarding the calculation of ion mobility

As its name suggests, IMS instruments use the mobility transport property of the ions to separate them in the gas phase. This is done by means of an electric field that acts on the ion. Including relaxation and orientation effects, the ion's momentum equation may be given by Ref. [11]:

$$M\overset{\dots}{\overrightarrow{x}} = q\overset{\longrightarrow}{E}(\overrightarrow{x},t) - \overline{\overline{B}}(\overrightarrow{x},t)\overset{\longrightarrow}{\overrightarrow{x}}. \tag{1}$$

Here, M is the mass of the ion, \overrightarrow{x} is the ion's instantaneous acceleration, q is its charge, $\overrightarrow{E}(\overrightarrow{x},t)$ is the electric field which may depend on position and time, \overline{B} is the rigid-rotor drag tensor assuming a Mason-Monchick approximation (the relative orientation is kept fixed during a collision) [8] and \overrightarrow{x} is the ion's instantaneous velocity. Note that the second term on the right-hand side of eq. (1) is averaged over all collisions and angles. This tensorial notion is used to state that velocity, field, and acceleration do not need to be instantaneously in the same direction. Assuming that all orientations are equally probable, a more than likely scenario, then it is expected that the average velocity is in the direction of the field and the tensor may be written as a scalar. Moreover, ignoring relaxation effects for the time being, $\overrightarrow{x} \sim 0$, eq. (1) becomes the typical assumption for mobility in kinetic theory [2]:

$$v_d = KE, \tag{2}$$

where v_d is the average drift velocity over time, and K is the mobility. Here the vectors have been dropped so that v_d is assumed to be in the direction of the field. Despite the numerous simplifications already present, it is well known that under constant fields and sufficiently small ions that do not suffer from non-inertial effects, eq. (2) is accurate to a fraction of a percent and may be used to calculate mobility in IMS systems. However, the equation by itself is insufficient to calculate the mobility theoretically as the drift velocity must be inferred for every ion. Kinetic theory or momentum transfer theory may be used to obtain the Mason-Schamp equation for zero field over concentration (E/n) at the gas temperature $T_0[5]$:

$$K_{1T}\left(T_0, \frac{E}{n} \to 0\right) = \frac{3}{16} \frac{ze}{n} \left(\frac{2\pi}{\mu k T_0}\right)^{1/2} \frac{1}{\overline{\Omega}_{T_0}(1, 1)}$$
 (3)

Here, ze is the charge of the ion, μ is the reduced mass, n is the gas number density, k is the Boltzmann constant and $\overline{\Omega}_{T_0}(1,1)$ is the orientationally averaged momentum transfer collision integral calculated at the gas temperature T_0 and which in IMS is referred to as the Collision Cross Section (CCS). It can be shown that $\overline{\Omega}_{T_0}(1,1)$ may be written as [2,10]:

$$\begin{split} \overline{\Omega}_{T_0}(1,1) &= \frac{1}{8\pi^2} \int\limits_0^{2\pi} d\theta \int\limits_0^{\pi} sin\varphi d\varphi \int\limits_0^{2\pi} d\gamma \frac{\pi}{8} \left(\frac{\mu}{kT_0}\right)^3 \int\limits_0^{\infty} g^5 e^{-\frac{\mu g^2}{2kT_0}} dg \\ &\times \int\limits_0^{\infty} 2b(1-\cos\chi) db \end{split} \tag{4}$$

In this equation, θ , φ and γ are the 3 orientation angles of the molecule, g is the relative velocity between gas and ion, b is the impact parameter and χ is the deflection angle. Note that the same assumption has been made here as when going from eq. (1) to eq. (2) where all orientations are equally probable. The deflection angle χ refers to the difference in trajectory after a gas molecule interacts

with the ion. Given that the ion-gas interaction physically involves a complex potential energy, the deflection angle is quite hard to calculate accurately even for the simplest of ions and is generally given by Ref. [12]:

$$\chi = \pi - 2b \int_{r_m}^{\infty} \frac{dr}{r^2 \sqrt{1 - \frac{b^2}{r^2} - \frac{2\Phi(r)}{\mu g^2}}}$$
 (5a)

where r_m is the apsidal distance. In IMS, calculation of eq. (5a) is done almost exclusively numerically [13–17]. For molecular ions, it generally involves the assumption of a simplified potential interaction $\Phi(r)$. Generally, the interaction potential used includes a Lennard-Jones (LJ) potential between individual atoms and gas molecules as well as an ion-induced dipole potential due to the presence of charges in the ion [13]:

$$\begin{split} &\Phi(x,y,z) = 4\varepsilon \sum_{i=1}^{\kappa} \left[\left(\frac{\sigma}{r_i} \right)^{12} - \left(\frac{\sigma}{r_i} \right)^{6} \right] \\ &- \frac{\alpha_p}{2} \left(\frac{ze}{\kappa} \right)^2 \left[\left(\sum_{i=1}^{\kappa} \frac{x_i}{r_i^3} \right)^2 + \left(\sum_{i=1}^{\kappa} \frac{y_i}{r_i^3} \right)^2 + \left(\sum_{i=1}^{\kappa} \frac{z_i}{r_i^3} \right)^2 \right], \end{split} \tag{5b}$$

being $r_i=(x_i,y_i,z_i)$ a relative distance between each of the κ atoms (and/or charges where it is assumed that partial charges are calculated for each atom). ε and σ are the typical LJ parameters of potential well-depth and zero-crossing, and α_p is the polarizability of the gas. Eqs. (4) and (5) lay out that the deflection angle will have a strong dependence on the gas and its temperature T_0 . While eqs. (3)–(5) are already quite numerically involved, they are simplifications of a much denser theory that will be expanded and physically reasoned in the following sections.

Since mobility is also dependent on gas density, it is customary to define a reduced mobility value at a standard pressure and density that may be used to compare different mobility results more accurately:

$$K_0\left(T_0, \frac{E}{n}\right) = K\left(\frac{P_0}{101325}\right) \left(\frac{273.15}{T_0}\right) = \frac{nK}{N_0}$$
 (6)

Here P_0 and T_0 are the pressure and temperature at which the mobility K was calculated and N_0 is the density of an ideal gas at standard pressure and temperature.

3. The physical calculation of the ion's velocity distribution and mobility

If not acquainted with kinetic theory, one would initially like to understand why the quadrature in eq. (3) is suitable for the calculation of mobility in IMS. As such, one must first introduce how the equation is derived. While the physical notion of how the ion interacts with the bath of gas when subject to the presence of an electrical field is quite straight forward and does not need further explanation, the modeling of such an effect is by no means simple and simplifications must be made [2]:

 Among the most notable simplifications lies the notion that the ion-neutral interaction lies within the free molecular regime, where it is assumed that the ion does not substantially perturb the gas. Given the dependence of the regime on the Knudsen number, whether the system is in the free molecular regime ultimately depends on the size of the ion, its relative velocity, the gas temperature and neutral concentration [18].

- 2) The number density of molecular ions is small enough that there will be negligible interaction between them so that space charge may be neglected.
- 3) While it could be reasoned in 1), the expectancy is that, in the free molecular regime, a three-body collision is very rare and can be neglected. This can be understood as the gas moleculeion collision is sufficiently short-lived and does not condense onto the ion. Even if the three-body collision might happen on larger ions, the effect can probably be divided into two separate collisions.
- 4) There is no gas density gradient, and the ion velocity distribution does not vary with time or does so in a quasi-steady way (such as in a T-wave system). This restricts any possible space and time variations of the distribution. It can also be assumed that the gas velocity follows a Maxwell-Boltzmann distribution.
- 5) Both entities, atom and gas, are assumed to be either monoatomic or rigid and non-rotating during a collision, so that internal rovibrational degrees of freedom can be initially excluded from the equation, although their effect will be introduced later on.

While momentum transfer theory can be used to obtain eq. (3) [12], it is more practical to obtain it by solving moments of the Boltzmann equation subject to constraints 1–5, which allows to obtain the drift velocity, ion's energy, diffusion coefficients and other parameters. Without going into details about how to obtain the Boltzmann equation, one can generally write it as [7]:

$$\left[\frac{\partial}{\partial t} + \overrightarrow{c} \cdot \nabla + \frac{ze\overrightarrow{E}}{M} \cdot \nabla_{\overrightarrow{c}}\right] f(\overrightarrow{r}, \overrightarrow{c}, t) = n\Im f(\overrightarrow{r}, \overrightarrow{c}, t), \tag{7a}$$

where the collision operator $\Im f(\overrightarrow{r}, \overrightarrow{c}, t)$ is given by:

$$\mathfrak{F}(\overrightarrow{r}, \overrightarrow{c}, t) = \iiint \left(f'(\overrightarrow{r}, \overrightarrow{c}', t) f'_{gas}(\overrightarrow{r}, \overrightarrow{c}'_{gas}, t) - f(\overrightarrow{r}, \overrightarrow{c}', t) f_{gas}(\overrightarrow{r}, \overrightarrow{c}'_{gas}, t) \right) gbdbd\varepsilon d\overrightarrow{c}'_{gas}$$
(7b)

Here \overrightarrow{c} and \overrightarrow{c}_{gas} are the velocities of the ion and gas and $f(\overrightarrow{r}, \overrightarrow{c}, t)$ and $f_{gas}(\overrightarrow{r},\overrightarrow{c}_{gas},t)$ are the ion and gas velocity distributions. The equation states that variations of the ion's velocity distribution in time and position and velocity spaces are brought about by the collision operator $\Im f(\overrightarrow{r},\overrightarrow{c},t)$. ε represents the out of plane angle of the collision between gas and ion that had been integrated previously in eq. (3) because $(1-cos\chi)$ was independent of it, which might no longer be the case here. The collision operator indicates that a particular velocity class of the ion between \overrightarrow{c} and $\overrightarrow{c} + d\overrightarrow{c}$ may be replenished through ion-neutral collisions of ions with velocities c' and c'_{gas} or may be lost through ion-neutral collisions of ions with velocities c and c_{gas} , taking into account that all gas velocities and trajectories as sampled. Through classical mechanics arguments and the existing potential interactions, one can show that a relation between primes and non-primes can be calculated. This relation is what makes the deflection angle appear in eq. (4).

Using the simplifications from 1-5 and assuming that the electric field lies in one single direction (e.g., x) then eq. (7a) may be written as [10]:

$$\frac{zeE}{Mn} \frac{\partial f(\overrightarrow{c})}{\partial c_{x}} = \Im f(\overrightarrow{c})$$
 (8)

where c_x corresponds to the ion's velocity in the x direction (aligned with the field).

If both distributions, ion and gas, were to be Maxwellian, eq. (7b) can be shown to be 0, e.g., under equilibrium. However, the presence of the electric field perturbs this equilibrium and therefore a new velocity distribution for the ion needs to be sought. Solving the Boltzmann equation, even with existing simplifications is quite complex. Instead, one can resort to solving moments of the equations. For this approach, one multiplies eq. (8) by a function of the ion's velocity, $\psi(\overrightarrow{c})$, and integrates over all possible ion velocities. By doing so, average quantities may be obtained of the type:

$$\langle \psi \rangle = \int f \psi(\overrightarrow{c}) d\overrightarrow{c} \tag{9}$$

This is accomplished in eq. (8) by using integration by parts on the left-hand side and the adjoint property of linear operators on the right leading to Ref. [2]:

$$\frac{zeE}{Mn} \int f \frac{\partial \psi}{\partial c_x} d\overrightarrow{c} = \iiint f f_{gas} (\psi' - \psi) gbdb d\varepsilon d\overrightarrow{c}_{gas} d\overrightarrow{c}$$
 (10a)

Or

$$\frac{zeE}{Mn} \left\langle \frac{\partial \psi}{\partial c_x} \right\rangle = \langle \Im \psi \rangle \tag{10b}$$

To obtain a suitable solution for eq. (10b), the method of weighted residuals may be used. The ion distribution is assumed then to be of the type:

$$f = f^{(0)} \sum_{l,r} c_{l,r} \psi_{l,r}(\overrightarrow{c}) \tag{11}$$

The functions $\psi_{l,r}(\overrightarrow{c})$ are chosen to be basis functions, so that $f^{(0)}$ is the weight function to the orthogonal product:

$$(\psi,\varphi) = \int f^{(0)} \psi \varphi d \, \overrightarrow{c} \tag{12}$$

The weight function turns out to be quite important to arrive at quadratures that are useful and do not numerically diverge when approximations are used. As an example, for zero and weak fields, the Chapman-Enskog approximation can be used, and the weight function may be assumed to be the Boltzmann distribution:

$$f^{(0)} = \left(\frac{M}{2\pi kT_0}\right)^{3/2} e^{-\frac{M(\overrightarrow{C})^2}{2kT_0}} \tag{13}$$

A set of the typical functions that satisfy the orthogonal product subject to the weight function are known as the Burnett functions given by:

$$\psi_l^{(r)}(\overrightarrow{c}) = \left(\frac{Mc^2}{2kT}\right)^{\frac{1}{2}} P_l\left(\frac{c_x}{z}\right) S_{l+\frac{1}{2}}^{(r)}\left(\frac{Mc^2}{2kT}\right)$$

where $S_{l+\frac{1}{2}}^{(r)}$ are the associated Laguerre polynomials and P_l are the Legendre polynomials [10]. Furthermore, one can express the linear collision operator through a series as:

$$\Im \psi_{l}^{(r)} = \sum_{s} a_{rs}(l) \psi_{l}^{(s)} \text{ with } a_{rs}(l) = \frac{\left(\psi_{l}^{(s)}, \Im \psi_{l}^{(r)}\right)}{\left(\psi_{l}^{(s)}, \psi_{l}^{(s)}\right)}$$
(14)

Introducing eq. (14) into eq. (10) allows the equation to be reduced to a set of integral quadratures belonging to the calculations of the $a_{rs}(l)$ terms. A first simplification could be done by reducing to a single term the summation of eq. (14), i.e., $a_{00}(1) \psi_1^{(0)}$.

With this approximation obtained, it can be shown that, through the recursiveness of the associated Laguerre and Legendre polynomials [10,12], an equation can be obtained that provides subsequent approximations through previous ones:

$$\begin{split} \left(l + \frac{1}{2}\right) a_{rr}(l) \left\langle \psi_{l}^{(r)} \right\rangle_{\eta} \\ &= \left(\frac{zeE}{Mn}\right) \left(\frac{M}{2kT}\right)^{\frac{1}{2}} \left[l\left(l + \frac{1}{2} + r\right) \left\langle \psi_{l-1}^{(r)} \right\rangle_{\eta-1} \\ &- (l+1) \left\langle \psi_{l+1}^{(r-1)} \right\rangle_{\eta-1}\right] - \left(l + \frac{1}{2}\right) \\ &\times \sum_{s=0}^{\eta+r-1} (1 - \delta_{rs}) a_{rs}(l) \left\langle \psi_{l}^{(r)} \right\rangle_{\eta-1}; \, \psi_{l}^{(-1)} = 0 \end{split}$$

where η corresponds to the approximation (and $\eta-1=1$ on the first approximation).

Given that
$$\psi_1^{(0)}=\left(\frac{M}{2kT}\right)^{1/2}c_x$$
, $\psi_0^{(0)}=1$, and $\left\langle \psi_1^{(0)}\right\rangle=\left(\frac{M}{2kT}\right)^{1/2}\nu_d$, the first approximation yields:

$$\langle K \rangle_I = \frac{e}{Mn} \frac{1}{a_{00}(1)} \tag{16}$$

Eq. (16) is the equivalent of equation (3) once the quadrature from $a_{00}(1)$ has been evaluated and the CCS can be seen as the momentum transfer moment.

Higher approximations can be obtained using eq. (15). For example, the 4th approximation would be given by:

$$\langle K \rangle_{IV} = \langle K \rangle_I \left[\alpha_0 + \alpha_1 \left(\frac{E}{n} \right)^2 + \alpha_2 \left(\frac{E}{n} \right)^4 + \alpha_3 \left(\frac{E}{n} \right)^6 + \dots \right]$$
 (17)

Here the α_i coefficients are complicated functions of the $a_{rs}(l)$ quadratures and the mass of the ion and gas. Eq. (17) also shows that mobility is a function of even powers of the field over concentration and that even at zero fields, eq. (16) is still an approximation, since α_0 is not necessarily 1 [5]. A problem with eq. (17) is that the field terms are not bounded, so the series eventually diverges with an increase in the field and should only be used for low fields. It is customary to make the terms dimensionless so that, for

example, the second term may be written as:
$$\alpha_1'\left(\frac{\varepsilon}{a_{00}(1)}\right)^2$$
 with $\varepsilon=$

 $(eE/Mn)(M/2kT_0)^{1/2}$. This allows for asymptotic relations to be obtained. This form tells us that the E/n competes with $T_0\Omega(1,1)$ and which establishes a minimum threshold to neglect higher order terms, and which depends on temperature.

Higher order moments may be used to obtain ion's other properties. An important one is the ion's kinetic energy which may be extracted from $\left\langle \psi_0^{(1)} \right\rangle_I = \left\langle \frac{3}{2} - \frac{Mc^2}{2kT} \right\rangle_I$. When calculated, an important equation that is generally ignored in IMS may be provided. This equation which was first introduced by Wannier shows [19]:

$$\frac{1}{2}M\left\langle c^{2}\right\rangle _{I}=\frac{3}{2}kT_{0}+\frac{1}{2}M\left\langle v_{d}\right\rangle _{I}{}^{2}+\frac{1}{2}m\left\langle v_{d}\right\rangle _{I}{}^{2}=\frac{3}{2}kT_{b},\tag{18a-b}$$

where $\langle c^2 \rangle$ is the average of the square of the thermal velocity of the ion and $\langle v_d \rangle_I$ is to represent that the drift velocity is obtained using a first approximation (such as the one from eq. (16)). In this

equation, the ion's energy is composed of three terms, the thermal energy of the ion $\frac{3}{2}kT_0$, the kinetic energy corresponding to the electric field, $\frac{1}{2}M\langle v_d\rangle_l^2$, and a portion of the electric energy which, due to the collisions with the gas, is transformed into randomized energy, $\frac{1}{2}m\langle v_d\rangle_l^2$ (widening the ion velocity distribution as will be shown later). Under low velocities, eq. (18a) may be reduced to its first or perhaps first and second term (if the mass of the ion is large enough). However, once the drift velocity becomes noticeable, i.e., with an energy comparable to the thermal energy of the gas, the initial approximation of eq. (16) is no longer valid. To comply with eq. (18b) a temperature for the ion, different from the gas must be employed, and advanced here as T_b . This will lead to the two-temperature theory.

Before we continue with the two-temperature theory, however, one can start to physically imagine how the ion, subject to an electric field is continuously accelerating, and is slowed down (perhaps sometimes sped up) by collisions with the gas. To show this physically, our group has developed IMoS 2.0, which is a Monte Carlo type algorithm that calculates mobility by assuming an NVT ensemble of gas molecules and ion. The ion can be subjected to an electric field, constant or varying in position and time. When a gas molecule enters the domain of influence of the ion, the interaction between gas and ion is observed. This interaction can be simulated with different degrees of complication, from assuming the ion as a simple hard sphere, through the inclusion of attractive and repulsive potentials, to the inclusion of internal degrees of freedom, rotation, and vibration, as well as preferred orientations. This simulation has the advantage that it is simple to show some physical aspects of mobility that are not understood from the quadrature integrals. It has the disadvantage that it requires a much larger sample population to get accurate results (sometimes billions of collisions are required).

One can test the simulation with a couple of simple calculations. Let us imagine, to begin, that an ion with a mass of 2880Da is subject to a constant electric field of 40Td in the X direction. The ion is simulated as a rigid body that can rotate (no vibration). The gas is assumed to be monoatomic, and collisions between gas and ion, are assumed to be specular where a hard-sphere potential is employed. One is only interested in observing the general results that can be obtained for the time being, so the geometry of the ion is somewhat unimportant. The simulation is run for several microseconds and the results shown in Fig. 1.

Fig. 1A graphs the instantaneous ion velocity in the X, Y and Z directions as a function of time. The velocity varies significantly in all directions but has an average value in the X direction, which corresponds to the drift velocity, and an average of zero in the Y and Z directions. Given, the large number of collisions, an inset shows how the ion behaves during 5ns of flight time. The ion is accelerating linearly in the X direction due to the field, while colliding with gas molecules (from the front and the back) until an equilibrium is reached at which the momentum transfer per unit time of the collisions equals the electric force on average. At this point, the mobility can be obtained using eq. (2). An ion velocity distribution may be obtained from the data as shown in Fig. 1B. The shape of this distribution depends on the energy of the collisions due to the field as extracted from eq. (18). At zero and very weak fields, the expectancy is that the velocity distribution in the X direction is symmetric with a low effect from the field. Given that the average velocity for Y and Z must be zero, it can be shown that the ion velocity distribution at zero field may be approximated by:

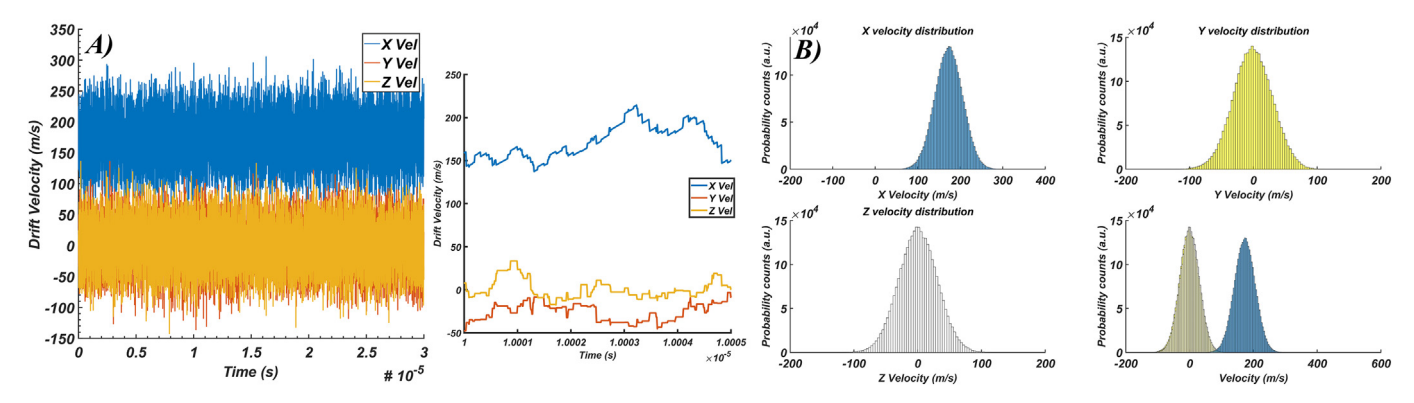


Fig. 1. A) Instantaneous ion velocity as a function of time in the X, Y and Z directions. The inset shows 5ns of flight time. B) Velocity distributions in the X, Y and Z directions using the raw data from Fig. 1A.

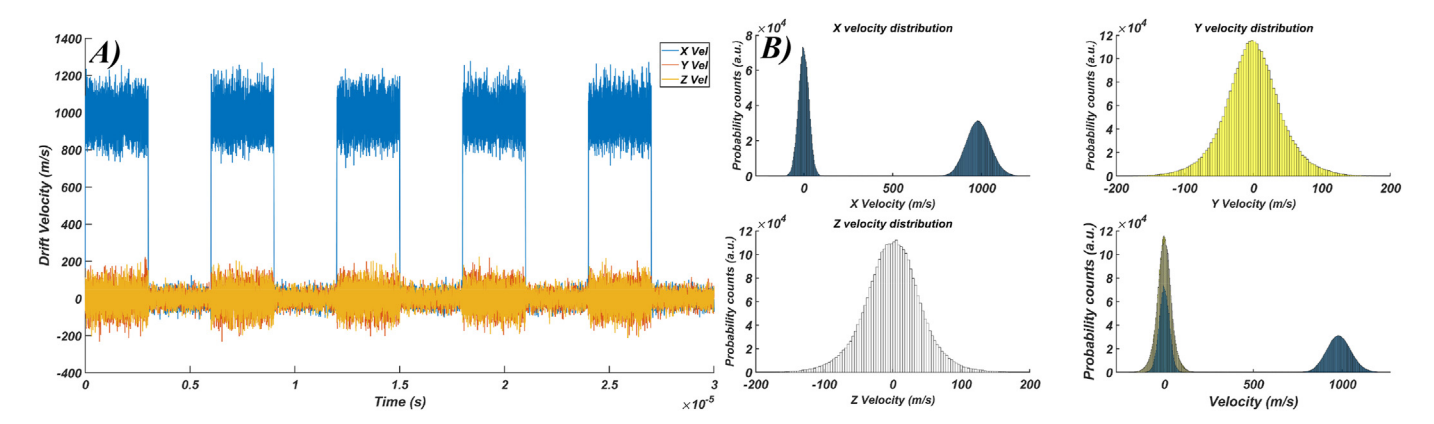


Fig. 2. A) Instantaneous ion velocity as a function of time in the X, Y and Z directions for a time-dependent field. B) Ion velocity distributions in the X, Y and Z directions using the raw data from Fig. 2B.

$$f\left(\overrightarrow{c}, \frac{E}{n} \to 0\right)_{M \gg m} = \left(\frac{M}{2\pi k T_0}\right)^{3/2} e^{-\frac{M\left(\overrightarrow{C} - \overrightarrow{\nu}_d\right)^2}{2k T_0}},\tag{19}$$

which is similar to a Maxwell distribution, but which is skewed in the direction of the drift velocity. This distribution can be shown to only work at low fields and for relatively large ions, but very useful nonetheless as a first approximation. The standard deviation of the distribution in eq. (19) is the typical Maxwellian $\sqrt{kT/M}$. However, even at the 40Td used, the width of the distributions is larger than the typical one (expected thermal-only FWHM is 69.28 m/s compared to the numerical 71.85 m/s in the Y and Z direction and 76.26 m/s in the X direction). This widening comes from the effect of the $1/2m\langle v_d\rangle_I^2$ energy term in eq. (18) and, while small here, becomes more relevant at higher fields (as shown below). It is therefore clear that the gas temperature T_0 employed in eq. (19) is ill-suited for high fields and an effective temperature may be used instead to take this into account. This effect is more pronounced in the X direction than in the Y and Z direction which suggests that perhaps different temperatures have to be used in the transversal and longitudinal directions. It also suggests that the diffusion coefficients may also be different.

To observe the effect of high fields and of relaxation, one can run the simulation with a varying field. To enhance the difference between high and low fields, the high field over concentration is increased to $400Td (10^4 \text{ V/cm})$, which, although somewhat high for IMS systems, is used here to intensify the effect. As the inertia

depends on the mass of the ion, it is expected that larger ions will suffer more from this effect so the heavy 2880Da ion is used with a high field mobility of 1000 (ms⁻¹)/1e6Vm⁻¹~1e-4 m²/Vs. Fig. 2A shows the result of a squared time-dependent field as the ion travels through the system. Every $3\mu s$, the field is instantly raised or lowered, leading to the pattern observed. The distribution in the X direction now becomes bimodal as is shown in Fig. 2B, as the average drift velocity varies between a low and a high value. The standard deviation changes can also be observed in both the X and Y/Z directions, where the distribution widens with higher fields due to the increase in collisional energy. There is also a difference between the X and Y/Z directions at high fields which once again suggests that the effective temperatures in the X and Y/Z direction must be different between each other and different from the gas temperature. Although difficult to see from the figure, the high field velocity distribution mode in the X direction is also not fully symmetric, with a slightly more prolonged tail towards higher velocities.

This particular field configuration may also serve the purpose of studying relaxation effects as shown in Fig. 3, where the ion acceleration and deceleration are zoomed in. Note how both effects seem to cancel each other out at least partially. In order to compare the effects of the simulation to theory, one can attempt to solve eq. (1) analytically. This may be done as an approximation by assuming the mobility to be a constant value (the high field value) and solving the differential equation. The analytical velocity results depending on whether the ion is accelerating or decelerating are given by:

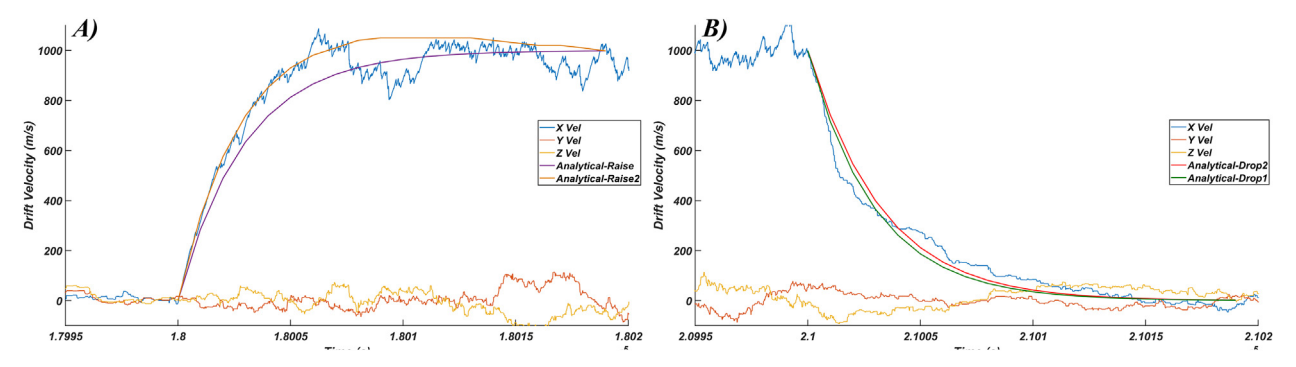


Fig. 3. Inset of Fig. 2A where A) the raise to high field or B) the drop to zero field is located. Analytical solutions are shown for constant and varying mobilities, where the 2 in the legend refers to a calculation with the mobility varying.

$$\dot{x}_{acel}(t) = \mathit{KE}\left(1 - e^{-\frac{ze}{\mathit{KM}}\left(t - t_0\right)}\right); \\ \dot{x}_{decel}(t) = \mathit{KE}e^{-\frac{ze}{\mathit{KM}}\left(t - t_0\right)}, \tag{20}$$

where t_0 represents the position where the field was raised or lowered. These analytical results are plotted on top of the simulation results in Fig. 3. While they are not expected to be exact, since the mobility should vary about 30%, the results approximately follow the expected trends. An alternative analytical derivation is shown assuming that the mobility decreases (with a power law) from 1.2e-4 m²/Vs to 1.0e-4 m²/Vs as the field is increased (or the opposite when it drops). How the mobility varies with the field is the subject of the following sections.

One of the reasons for this numerical exploration was to enable the possibility of making an informed guess about how the distributions may look as one increases the field. As the ion accelerates and achieves higher drift velocities, the collisions are certainly more energetic, since the relative velocity between gas and ion increases. As such, the ion temperature, T_h , may be regarded to be different than the gas. It should then be expected that at least the standard deviation of the distribution in eq. (19) has to be increased by an amount that is somewhere between the ion and the gas temperature. It can be shown that this temperature is given by an effective temperature, T_{eff} . It is also interesting to note that the temperature effect is shown to be different in the axial and transversal directions so a different effective temperature in the X direction, T_L , than in the Y and Z directions, T_D could be employed. A final note, when high fields are present, it is expected that the distribution will no longer be symmetric.

Regarding varying field systems, i.e., T-wave, simulations show that the theoretical analysis may become more problematic as the ion's velocity distribution becomes a complicated mixture of low and high fields that is difficult to analyze theoretically, even when the relaxation effects are ignored.

The possibility of some of the kinetic energy of the collisions to go into rovibrational degrees of freedom of both ion and gas producing what are known as inelastic collisions has not been discussed yet. This brings the possibility for ion and gas of having a different internal temperature T_i . These inelastic collisions are expected to be more prevalent at higher fields and for heavier ions and molecular gases and will be introduced in the next sections.

As can be seen from these two examples, the capabilities of the software are rather extent, but it requires significant computer power to be run efficiently. To put things into perspective, if one were to reduce the field to a value close to zero, the distribution would almost be Maxwellian and given by eq. (19). If one were to center the system on the ion and calculate the fluxes of gas molecules that enter the domain of the ion, the program would yield the

non-linearized results from IMoS, a program which has been extensively validated [16,17,20,21].

Given the dependence on the strength of the field over gas density and the temperature of the gas, a suggestion is made based on previous protocols that mobility should be described by two terms, T_0 and E/n as well as the gas employed and the instrument involved (in case relaxation effects are to be included), i.e., $K_{T-wave}^{He}\left(T_0,\frac{E}{n}\right)$.

4. Advanced theoretical methods for calculating mobility

Now that the basics of mobility have been established and that an idea of how an ion behaves in the presence of an electric field has been introduced, one can start to describe some of the more theoretically advanced interpretations of mobility. Only a brief introduction of the methods and useful numerical results will be highlighted, leaving the more sophisticated theoretical analysis to previous works from the author and others [2,4,12].

Given that at high fields, ion and gas can be observed to have different temperatures, the weight function or zero order function may be modified to Refs. [6,7]:

$$f^{(0)} = \left(\frac{M}{2\pi kT_b}\right)^{3/2} e^{-\frac{M(\overrightarrow{C})^2}{2kT_b}}$$

Using the same principle of weighted residuals and moment solutions as before, it can be shown that the mobility may be given by Refs [6.7].

$$K_{2T}\left(T_0, \frac{E}{n}\right) = \frac{3}{16} \frac{ze}{n} \left(\frac{2\pi}{\mu k T_{eff}}\right)^{1/2} \frac{1 + \alpha_c}{\overline{\Omega}_{T_{eff}}(1, 1)}$$
(21)

where the effective temperature T_{eff} is given by:

$$\frac{3}{2}kT_{eff} = \frac{3}{2}kT_0 + \frac{1}{2}mv_d^2(1+\beta_c)$$
 or

$$T_{eff} = \frac{MT_0 + mT_b}{m + M} \tag{22a-b}$$

In eq. (21), $\overline{\Omega}_{T_{eff}}(1,1)$ is calculated at the effective temperature. The terms α_c and β_c are corrections to the first approximation of the two-temperature theory. They are obtained similarly to those of eq. (17) and correspond to convoluted expressions of higher order collision integrals as well as the masses of ion and gas. For a thorough analysis of the two-temperature theory for molecular ions, ref. [14] is recommended. They correspond to values of

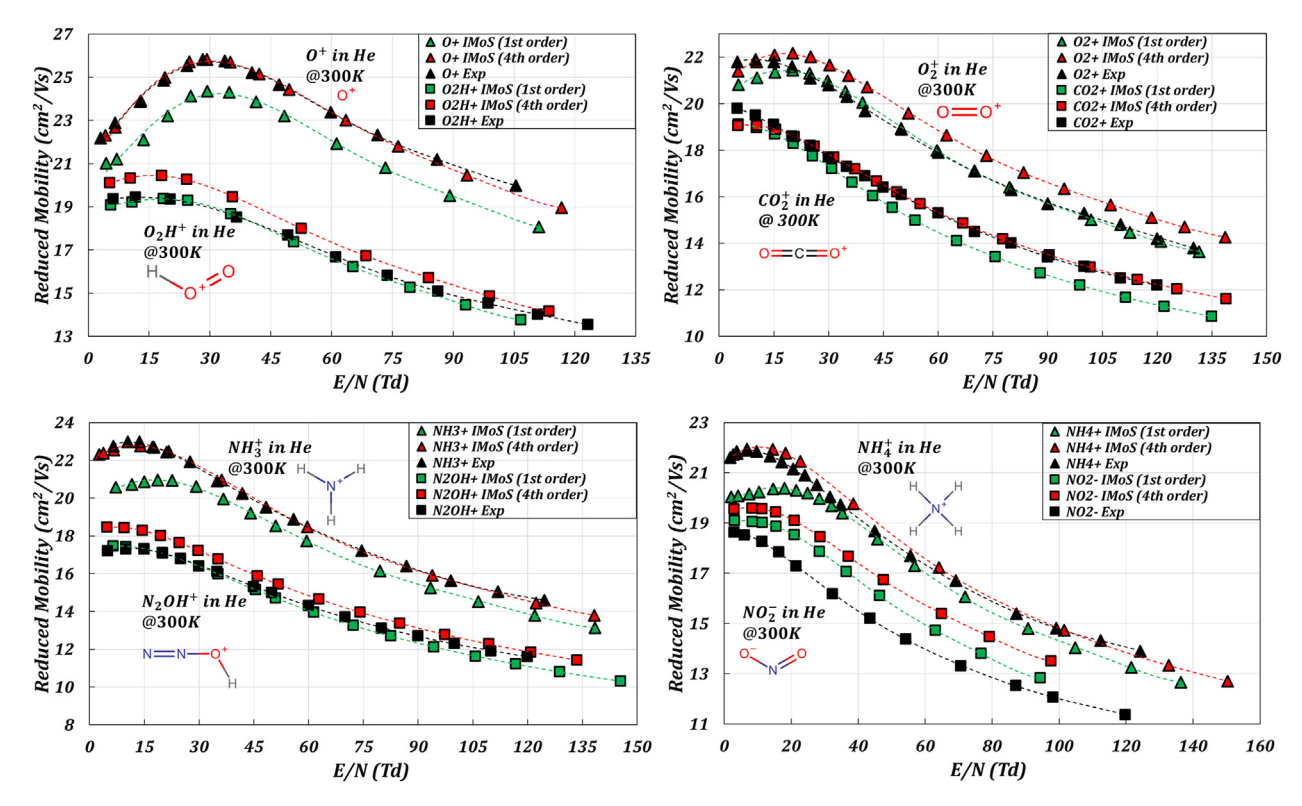


Fig. 4. Reduced mobility as a function of the field over concentration for a set of small ions in light gases using the two-temperature approximation in the 1st and 4th approximations. Extracted from Ref. [22].

approximately 0–0.2 depending on the field and reduced mass. Eqs. 21 and 22 are convoluted in the sense that the mobility K (through the drift velocity in eq. (22a)) and T_{eff} appear on both equations in a non-linear fashion. On the first approximation to the two-temperature theory, $\alpha_C = \beta_C = 0$, which makes eq. (21) almost identical to eq. (3) but where instead the effective temperature is employed. This small change allows calculations at high fields to be performed efficiently using zero field calculators by approximating the field through the effective temperature using eq. (22a). Eq. (21) does not diverge like eq. (17) so even the first approximation may be used for the whole field range expecting errors of 10% [7].

The α_c term, if its value is known as a function of the field, may later be added to the numerical calculation as a correction. This has been attempted in a recent work using IMoS for small ions in light gases with very promising results up to the 4th approximation, some of which are here reconstructed in Fig. 4 [22]. Mobcal results are equally applicable here, with the advantage that its structure easily allows higher order approximations to be constructed [13].

Kinetic theory studies go beyond the two-temperature theory into the three-temperature and multi-temperature theories as it can be shown that the two-temperature theory cannot describe transversal diffusion for ions appropriately [24–26]. Given the difficulty of experimentally calculating transversal temperatures and the fact that they do not shed any useful information into mobility, they have been left out of the scope of this work. An improvement over the two-temperature theory is the Gram-Charlier theory [27]. As indicated by Viehland, this approach was developed to counteract the arguments by Skullerud [28], who posed that the true ion velocity distribution should fall off more slowly than any gaussian distribution. The method consists of assuming a correction to the zero-order weight function distribution that accounts for kurtosis and skewness. The correction adds new coefficients to the distribution that can be argued to be

equivalent to results of high order moments, and thus a closed method is created that can only be solved numerically but that is expected to be more accurate than the two-temperature method. The Gram-Charlier method has been used on atomic ions in atomic gases successfully.

This provides further evidence of how mobility should be expressed and calculated experimentally. It is quite important that the gas temperature and the E/n at which the experiment was run is provided. Naturally, the neutral gas that was employed and the instrument, in case relaxation effects appear, used should also be indicated.

5. Potential interaction effects. Ab initio and quantum mechanical calculations

Most of the ions in Fig. 4 show that the reduced mobility has a hump-like behavior as a function of T_{eff} or E/n. The hump has been shown to be the effect of potential interactions between gas and ion. To understand how potential interactions may strongly affect mobility, in particular at low temperatures, it is best to first study the behavior of ions assuming a hard sphere model. From eqs. (6) and (21-22) and assuming that the collision cross section is given by $\overline{\Omega}_{T_{eff}}(1,1)=\pi d_{eff}^2$, one can write assuming $T_{eff}\gg T_0$:

$$K_{02T}\left(T_0, \frac{E}{n}\right) = \frac{1}{N_0} \left(\frac{6\pi}{m\mu(1+\beta_c)}\right)^{\frac{1}{4}} \left(\frac{3ze}{16} \frac{(1+\alpha_c)}{\pi d_{eff}^2}\right)^{1/2} \left(\frac{E}{n}\right)^{-1/2}$$
(23)

As can be observed, for a hard sphere model, the ion's reduced mobility decreases with the increase of the field to the -1/2. This was already observed by Patterson when calculating mobilities of the Helium ion [29]. Generally, however, the potential interaction

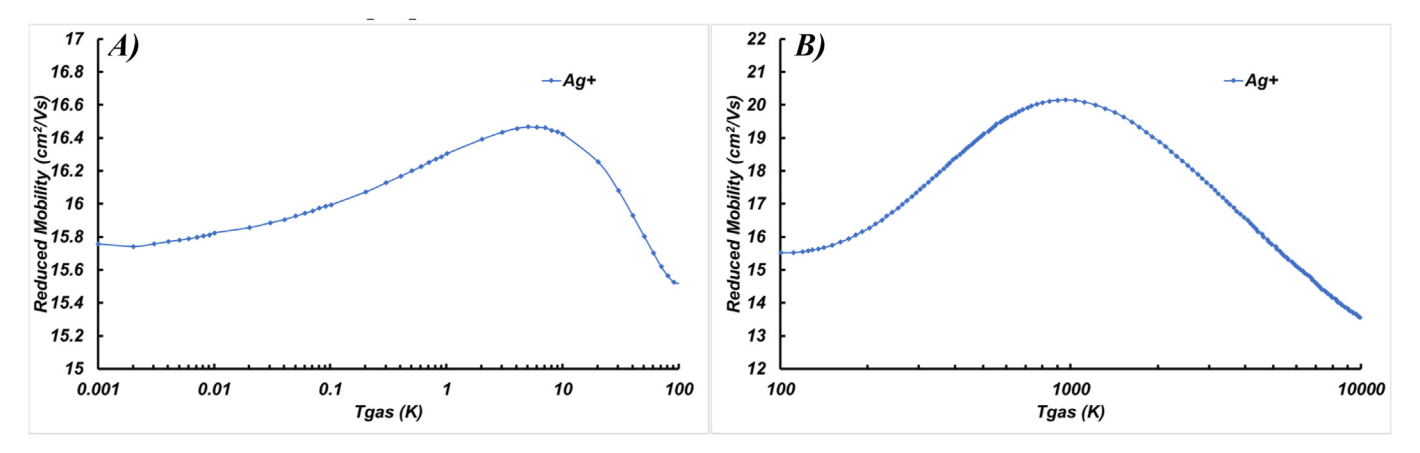


Fig. 5. Numerical calculation of Reduced mobility as a function of gas temperature for silver cations for A) 0.001–100 K and B) 100–1000 K.

for most ions is sufficiently large that this asymptotic behavior is rarely reached for most ions and fields, and a smaller power than -1/2 is expected (-1/4 to -1/3 is achieved for ions in Fig. 4).

The potential interaction becomes even stronger for small or heavily charged ions at low fields and/or temperatures which causes the reduced mobility graph to curve forming the hump that is visible at low fields. To show that a similar effect occurs with temperature, an example is given in Fig. 5 which provides the numerically calculated zero-field reduced mobility as a function of the gas temperature for the monoatomic silver ion A_g^+ 107 in He [30], for very low temperatures (0.001–100 K) (Fig. 5A) and low to high temperatures (100–10000 K) (Fig. 5B). While the effect for the latter is quite similar to what is observed for high fields, the effect of the former was calculated by using an ion-neutral potential obtained from ab-initio calculations [30].

At the limit of zero temperature and zero-field, due to the ioninduced dipole potential, there is a polarization limit which is given by:

$$K_0(0,0) = \frac{13.853 \, cm^2 / Vs}{\sqrt{\alpha_p \mu}} \tag{24}$$

and which would yield a value of $15.494 \, cm^2/Vs$ for the A_g^+107 ion in He, which is close to the calculation for low temperatures (in fact it is closer to the value at 100 K before other low temperature effects start appearing).

Given the ab-initio results from Fig. 5, a final point to address regarding potential interactions has to do with establishing whether or not the (4-6-12) potential interaction used in eq. (5) is accurate enough for our purposes. It has been shown that accuracies within a few percent (~4%) may be obtained using such potentials with optimized parameters [14,15,20,31]. Other basic potentials, e.g., Buckingham or ion-quadrupole potentials, may be used in a similar manner, but the accuracy is not expected to be substantially higher [14,32], as the mobility quadrature and interaction potentials are still approximations.

If one were to require more accurate potentials, an option is to resort to ab-initio calculations. In practice, the idea is that if the potential energy surface can be calculated from a quantum mechanical perspective using the best possible approach, there is no need to involve adjustable parameters, such as the potential-well and zero crossing, to determine the ion's mobility and the calculation can be done without the necessity of a comparison with experiments. As the deflection angle calculation in equation (4) depends on the potential energy interaction between gas and ion,

finding $\Phi(r)$ for the ion-molecule pair would be sufficient to accurately predict mobility without the need for adjustable parameters. Viehland and Chan developed a program labeled PC that is able to get a set of tabulated points $(\Phi(r), r)$ and use them to calculate eq. (3) and higher order collision integrals. The additional interactions allow more accurate calculations at low temperatures as shown in Fig. 5A. While the prospects are good for atomic (gas and ion) entities for which these ab initio calculations may be performed [33,34], the same cannot be said for large molecular entities given the computational requirements so they cannot be pursued as easily in IMS.

Quantum mechanical calculations for the momentum transfer cross section have been calculated by Viehland and Hurly and compared to classical calculations [35]. The differences are negligible except at very small collision energies where the quantum effects become important. For this reason, adding quantum calculations to IMS mobility results is not necessary at this point and will not be pursued here.

In all, given the similarities brought forward by the two-temperature theory through eq. (21), the effect of increasing the electric field in reduced mobility (not standard mobility) is mathematically very much similar to that of an increase in the gas temperature where an effective temperature is used to describe the collisional energy of gas and ion. However, the two-temperature theory is meant for atomic entities where no internal degrees of freedom are considered. In the case of polyatomic gases and ions, the difference may become notable at high fields, as part of the energy of the collisions may go into internal degrees of freedom (rovibrational), affecting the overall momentum transfer of the ion-neutral pair and hence the mobility. The loss of translational energy into other modes is referred to as an inelastic collision in kinetic theory.

6. Effect of inelastic collisions on molecular ions and gases

The theory presented so far in this work has been done assuming atomic entities, both for the gas and the ion. While at zero and weak fields, the results portrayed above may be used without loss of generality for molecular ions, one has to be careful if they are to be employed at higher fields. From a purely kinetic perspective, there is the expectancy that in an ion-gas collision, part of the collisional energy will go into heating the internal degrees of freedom and hence the collision can no longer be regarded as elastic.

An extension of the Boltzmann equation, the Wang-Uhlenbeckde Boer (WUB) equation, can be used to include the internal degrees of freedom, both rotational and vibrational, of ion and gas molecule [3]. The new equation describes the collisions between two particles with initial internal states α and β which change into internal states α' and β' . The equations do not vary significantly from those of eq. (21), aside from the addition of internal energies and the appearance of an "internal" temperature for the ion, T_i , which differs, in principle from T_b and T_{eff} . The momentum transfer collision integral may now be written as [2]:

$$\Omega_{T_0}^{(\alpha,\beta)}(1,1) = \frac{1}{ZZ_0} \sum_{\alpha\beta\alpha'\beta'} \int_0^\infty \int_0^{2\pi} \int_0^{2\pi} \times \int_0^\infty \gamma_r^5 e^{-\left(\gamma_r^2 + \frac{\epsilon_i^{(\alpha)}}{kT_i} + \frac{\epsilon_i^{(\beta)}}{kT_0}\right)} \left(1 - \frac{\gamma_r'}{\gamma_r} \cos\chi\right) d\gamma_r b d\epsilon db$$
(25a)

And where:

$$Z = \sum_{\alpha} e^{-\frac{e_i^{(\alpha)}}{kT_i}}; \ Z_0 = \sum_{\beta} e^{-\frac{e_i^{(\beta)}}{kT_0}};$$
 (25b-c)

$$\gamma_r^2 = \frac{\mu g^2}{2kT_{eff}} = \frac{\varepsilon}{kT_{eff}}; \ {\gamma_r'}^2 = \frac{\varepsilon'}{kT_{eff}} \ ; \ \varepsilon' - \varepsilon = \varepsilon_i^{(\alpha')} + \varepsilon_i^{(\beta')} - \varepsilon_i^{(\alpha)} - \varepsilon_i^{(\beta)} \endalign{\mbox{\ensuremath{g}}\mbox{\ensuremath{e}\mbox{\ensuremath{e}}\mbox{\ensuremath{e}}\mbox{\ensuremath{e}}\mbox{\ensuremath{e}}\mbox{\ensuremath{e}}\mbox{\ensuremath{e}}\mbox{\ensuremath{e}}\mbox{\ensuremath{e}}\mbox{\ensuremath{e}}\mbox{\ensuremath{e}}\mbox{\ensuremath{e}}\mbox{\ensuremath{e}}\mbox{\ensuremath{e}}\mbox{\ensuremath{e}}\mbox{\ensuremath{e}}\mbox{\ensuremath{e}}\mbox{\ensuremath{e}}\mbox{\ensuremath{e}}\mbox{\ensuremath{e}}\mbox{\$$

Here, the averaging over all orientations is omitted to avoid unnecessary cluttering (and hence the bar on top of Ω is removed even though it still is averaging over the rest of parameters). Z and Z_0 are the internal partition functions of ion and gas, and $\varepsilon, \varepsilon_i^{(\alpha)}$ and $\varepsilon_i^{(\beta)}$ are the total ion energy and internal energies of ion and gas respectively which include both rotational and vibrational degrees of freedom. The term $\left(1-\frac{\gamma_r'}{\gamma_r}cos\chi\right)$ is a correction of the momentum transfer that reflects the change in dimensionless relative velocity γ_r' after a collision, and hence the inelasticity in the collision. The sum $\sum\limits_{\alpha\beta\alpha'\beta'}\ldots$ together with the partition functions indicates that the

CCS calculation has to be done averaging over all possible internal states before and after the collision (which appear directly or indirectly through γ'_r and χ).

For monoatomic ions and gases, and for low fields, $T_i = T_{eff} = T_0$, and eq. (25a) reverts back to eq. (3). Under other scenarios, eq. (25a-f) should be used for polyatomic ions where a possibility exists that translational energy may be diverted into other degrees of freedom. Following a similar procedure to the one-temperature and two temperature theories, one can also obtain higher approximations and higher order moments. These higher moments are normally written as a function of irreducible integrals similar to the CCS and given by:

$$A = \frac{\pi^{-\frac{3}{2}}}{ZZ_0} \sum_{\alpha\beta\alpha'\beta'} \int_0^{\infty} \int_0^{2\pi} \int_0^{\infty} A(\overrightarrow{g})g\gamma_r^2 e^{-\left(\gamma_r^2 + \frac{e^{(\alpha)}}{kT_i} + \frac{e^{(\beta)}}{kT_0}\right)} d\gamma_r b d\varepsilon db$$
 (26)

For example, the mobility may then be given for the first approximation as:

$$\begin{split} \left\langle K^{(\alpha,\beta)} \right\rangle_{I} &= \frac{ze}{2\mu n \left\langle \left\langle \gamma_{r_{X}} \left(\gamma_{r_{X}} - \gamma_{r_{x}}^{\prime} \right) \right\rangle \right\rangle} \; ; \; \Omega_{T_{0}}^{(\alpha,\beta)}(1,1) \\ &= \frac{3}{8} \left(\frac{2\pi\mu}{kT_{eff}} \right)^{1/2} \left\langle \left\langle \gamma_{r_{X}} \left(\gamma_{r_{X}} - \gamma_{r_{x}}^{\prime} \right) \right\rangle \right\rangle \end{split} \tag{27a-b}$$

And the energy of the ion can be calculated in terms of the effective temperature (eq. (22b)) which yields:

$$\begin{split} \frac{3}{2}kT_{eff}\left(1+\frac{m}{M}\xi\right) &= \frac{3}{2}kT + \frac{1}{2}m\nu_{d}^{2}; \ \xi = \frac{\left\langle\left\langle\gamma_{r}^{2} - \left(\gamma_{r}^{'}\right)^{2}\right\rangle\right\rangle}{6\left\langle\left\langle\gamma_{r_{x}}\left(\gamma_{r_{x}} - \gamma_{r_{x}}^{'}\right)\right\rangle\right\rangle} \\ &= \frac{\left\langle\left\langle\varepsilon_{i}^{(\alpha')} + \varepsilon_{i}^{(\beta')} - \varepsilon_{i}^{(\alpha)} - \varepsilon_{i}^{(\beta)}\right\rangle\right\rangle}{6\left\langle\left\langle\gamma_{r_{x}}\left(\gamma_{r_{x}} - \gamma_{r_{x}}^{'}\right)\right\rangle\right\rangle kT_{eff}} \end{split}$$

$$(28a-b)$$

Here ξ is the fractional energy loss or gain due to inelastic collisions. It may be written as the ratio of internal energy loss to momentum transfer exchange. It is interesting to see that the difference in the energy equation with respect to monoatomic entities seems to come only through this ratio. As such, if $\xi=0$, eq. (28) reverts back to the first approximation in eq. (22a). However, one has to consider the fact that the drift velocity that appears in eq. (28a) will have inelastic effects through collision integrals such as eq. (25). Under most cases pertaining to IMS, ξ is not expected to be very large, except perhaps for very light ions in very heavy molecular ions and large fields. ξ is also pre-multiplied by the mass ratio m/M, so the effect becomes smaller for larger ions.

A particular issue for the irreducible integrals eqs. 25-28 is that they are function of the internal temperature T_i . As such, the internal temperature must be calculated before attempting to solve the quadrature. The internal temperature may be rationalized as the temperature at which the difference in internal energy between pre and post-collision is zero on average:

$$\left\langle \left\langle \varepsilon_{i}^{(\alpha)} - \varepsilon_{i}^{(\alpha')} \right\rangle \right\rangle = 0.$$
 (29)

There are special cases that are noteworthy such as when the ion or the gas are monoatomic. The case of atomic ions is straight forward as T_i disappears and the problem may be reverted back to the two-temperature theory, as interactions with molecular gases are not expected to vary significantly from those with atomic gases. The second case, molecular ions in atomic gases, in which $\varepsilon_i^{(\beta)}=0$, is a little more complex but with very interesting repercussions. Given that the energy modes of escape for translational and internal degrees of freedom of the ion is the same, i.e., the translational energy of the gas, it can be proven that $T_i=T_{eff}$, and eqs. (28b) and (29) become identical. This is one of the main reasons why the two-temperature theory works well for the small ions in He presented in Fig. 4. Even though some inelasticity may be present at high fields, it is not expected to be large. This certainly will be different in the case molecular gases.

Given that insufficient data is available to calculate ξ or compare numerical results to experiments at different fields or temperatures, and the difficulty concerning the number of internal states that would need to be calculated for any large molecule, there is still a lot of work to do before the WUB theory can be optimally used for IMS. An alternative option the WUB is to do Monte Carlo simulations that include internal degrees of freedom to study the effect such as those attempted in section 3 and expanded below.

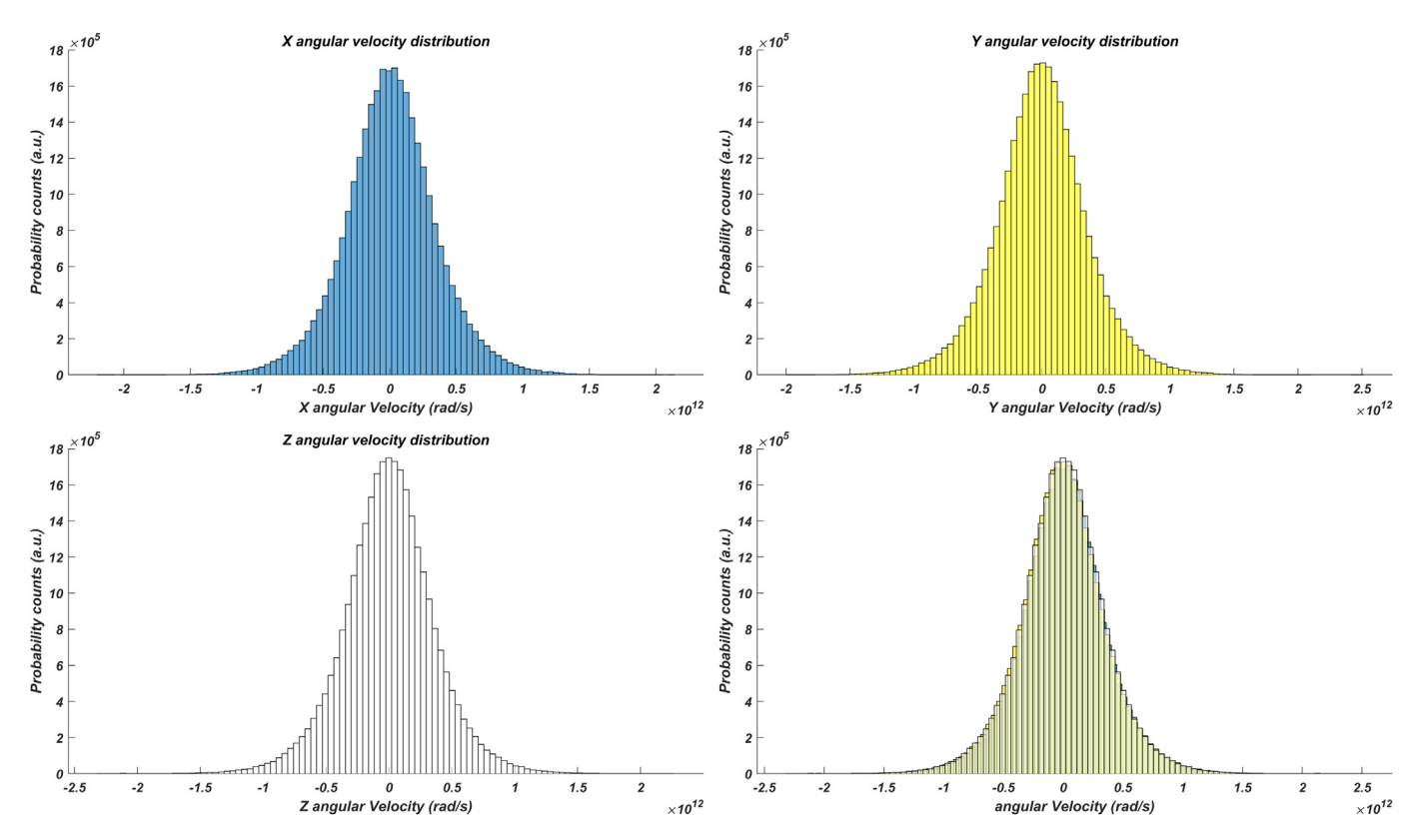


Fig. 6. Angular velocity distributions in the X, Y, Z global directions in the constant low field case.

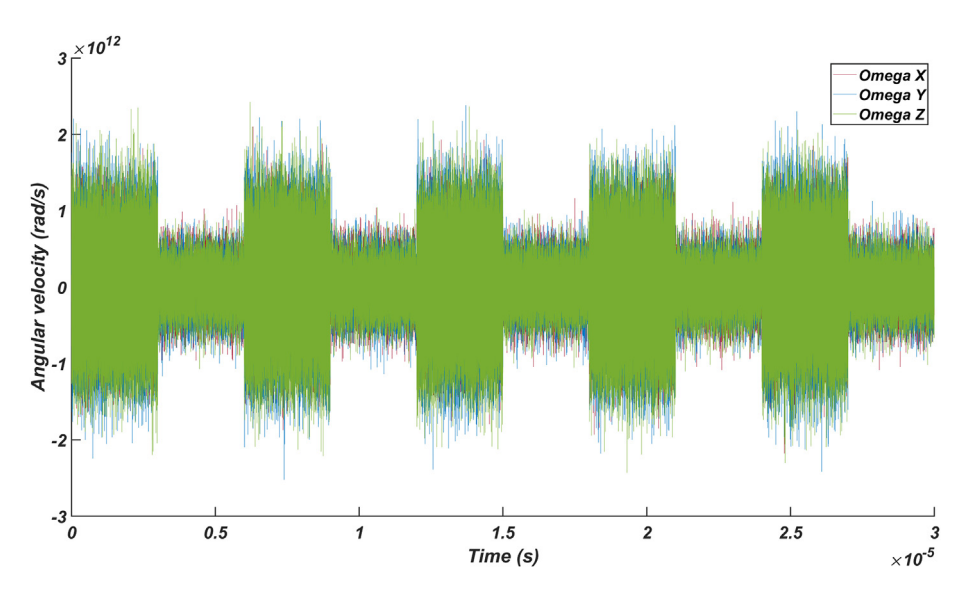


Fig. 7. Instantaneous angular velocity in global axes as a function time for the varying high field case.

7. Prediction of ion mobility through real-time Monte Carlo simulations

Given the difficulty of addressing IMS through the WUB equation, one must look for other means to overcome theoretical limitations. One of such methods is the Monte Carlo approach used above where a gas bath and an electric field are present. The interaction of the ion with the field happens at all times and positions. However, the interaction between the molecular ion and the gas molecule is restricted to the domain of influence (which

may have a cutoff if potential interactions are present). Once a gas molecule is in the domain of influence of the ion, one can describe the interaction with as many details as desired. The momentum transfer is calculated in real-time while ion and neutral interact until the gas molecule leaves the domain of influence. By using simplified cases of interactions, information may be obtained on their effect.

For example, one can use the study in section 3, to see how angular rotation is affected by the presence of the field and where no other internal degrees of freedom are employed. The results for

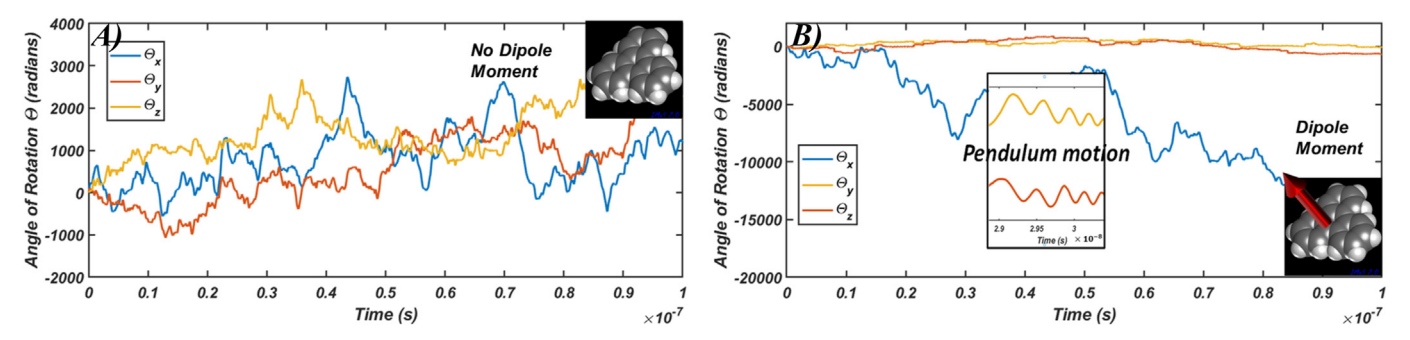


Fig. 8. Orientation angle as a function of time for a triphenylene molecule with A) no dipole moment and B) 100 Debye dipole moment. Inset shows that the ion orientation is constricted in two of the three directions. Extracted from Ref. [12].

the angular velocity distribution in global axes for the constant low field case are presented in Fig. 6 and the instantaneous angular velocity as a function of time for the varying high field case is presented in Fig. 7.

Fig. 6 shows that, in global axes, there is no specific preferred orientation for rotation and all angular velocity distributions are equal in all directions. This may be different in the object axes, however, as different moment of inertia in the different directions are expected to lead to different angular velocities. The varying field case in Fig. 7 sheds very important information for polyatomic ions. Some of the electric field energy is used to heat up the rotational degrees of freedom increasing the standard deviation of the distribution at high fields. From this heating, the internal equilibrium temperature T_i introduced in section 6 may be extracted, and which in this case, since the gas in monoatomic, is expected to be equivalent to the effective temperature T_{eff} . However, it would be wrong to completely expect the effective temperature to be exactly the same as in the two-temperature theory as inelasticity effects do come into play through v_d . Given a collision, therefore, there will be an exchange between the rotational degrees of freedom. This exchange will depend on the relative velocity, the Moment of Inertia (MoI) and the Center of Mass (CoM) of the ion. This suggests the possibility that isotopomer, ions which have identical structures and only differ in the distribution of heavy isotopes within the molecule, may be separated by IMS. This has been, in fact, recently observed in high resolution ion mobility devices such as Structure for Lossless Ion Manipulations (SLIM) and High Field Asymmetric Waveform Ion Mobility Spectrometry (FAIMS) [36–38]. Given these results, the Monte Carlo algorithm IMoS 2.0 from section 3 was employed to study the separation of tandem mass tag TMT and iodo-TMT isotopomers. The results from the simulation agree qualitatively with experiments not only in the magnitude of the mobility shifts but also the direction. By enabling the energy transfer between rotational and translational degrees of freedom, shifts in mobility can be traced back to the difference in MoI and CoM between isotopomers [39]. Adding vibrational degrees of freedom is expected to yield more information on inelastic collisions in the near future.

Finally, Monte Carlo simulations of this type can also be used to study effects of alignment which are not included in the general kinetic theory. In a case study, a triphenyline molecule was simulated with a constant field with and without the effect of a permanent dipole and the ability to rotate [12]. If the permanent dipole is sufficiently strong, the expectancy is that the system will try to align the dipole with the field. The result of the orientation angle of the molecule is extracted from the reference and presented in Fig. 8 for the case with and without the dipole. Fig. 8A shows what is typically expected of an ion without any means of alignment, that is, all orientations are equally probable, and the ion rotates

randomly. Fig. 8B, on the contrary, shows that the ion is constricted in two of the three directions due to the existence of a permanent dipole moment, and it is free to rotate on the third. The inset shows the typical torque overshoot characteristic of pendular motion along the stable position.

8. Conclusions

A perspective on the future of theoretical and numerical applications has been presented in a pedagogical fashion intended to explain the logic behind the quadratures obtained from kinetic theory. Full real-time simulations using IMoS 2.0 shed light into secondary effects in mobility, and higher order approximations for higher fields and temperatures. These Monte Carlo type simulations can be successfully used to describe all the effects envisioned in kinetic theory, albeit in a very numerically inefficient manner. In particular, emphasis is made on the effect that internal degrees of freedom may have on mobility calculations. It is clear that a mixture of both theory and this type of Monte Carlo simulations will provide a guideline for IMS in the future. A proposition is made to label results from experimental mobility (reduced mobility preferred) stating the gas temperature, the electric field at which the calculation was done, the gas or mixture of gases used, and the system employed (if non-constant fields are employed). An example of the labeling would be: $K_{0T-wave}^{He}\left(T_{0},\frac{E}{n}\right)$.

CRediT authorship contribution statement

Carlos Larriba-Andaluz: Conceptualization, Data curation, Formal analysis, Funding acquisition, Investigation, Methodology, Project administration, Resources, Software, Supervision, Validation, Visualization, Writing — original draft, Writing — review & editing.

Declaration of competing interest

The authors declare that they have no known competing financial interests or personal relationships that could have appeared to influence the work reported in this paper.

Acknowledgements

This work is supported by the National Science Foundation Division of Chemistry under Grant No. 1904879 (Program officer Dr. Kelsey Cook) and under Grant No. 2105929 (Program officer William Olbricht).

References

- [1] G.A. Eiceman, Advances in ion mobility spectrometry: 1980–1990, Crit. Rev. Anal. Chem. 22 (1991) 471–490
- [2] E.A. Mason, E.W. McDaniel, Transport Properties of Ions in Gases, John Wiley & Sons., New York, 1988.
- [3] G.E. Uhlenbeck, J. De Boer, Studies in Statistical Mechanics, 1962. North-Holland.
- [4] L.A. Viehland, L.A. Viehland, Gaseous Ion Mobility, Diffusion, and Reaction, Springer, 2018.
- [5] E.A. Mason, H.W. Schamp Jr., Mobility of gaseous lons in weak electric fields, Ann. Phys. 4 (1958) 233–270.
- [6] L.A. Viehland, E. Mason, Gaseous Ion mobility in electric fields of arbitrary strength, Ann. Phys. 91 (1975) 499–533.
- [7] L.A. Viehland, E. Mason, Gaseous ion mobility and diffusion in electric fields of arbitrary strength, Ann. Phys. 110 (1978) 287–328.
- [8] L. Monchick, E. Mason, Transport properties of polar gases, J. Chem. Phys. 35 (1961) 1676–1697.
- [9] H. Revercomb, E.A. Mason, Theory of plasma chromatography/gaseous electrophoresis, Rev. Anal. Chem. 47 (1975) 970–983.
- [10] T. Kihara, The mathematical theory of electrical discharges in gases. B. Velocity-distribution of positive ions in a static field, Rev. Mod. Phys. 25 (1953) 844.
- [11] C. Larriba-Andaluz, M. Nahin, V. Shrivastav, A contribution to the amaranthine quarrel between true and average electrical mobility in the free molecular regime, Aerosol Sci. Technol. 51 (2017) 887–895.
- [12] C. Larriba-Andaluz, J.S. Prell, Fundamentals of ion mobility in the free molecular regime. Interlacing the past, present and future of ion mobility calculations, Int. Rev. Phys. Chem. 39 (2020) 569–623.
- [13] M.F. Mesleh, J.M. Hunter, A.A. Shvartsburg, G.C. Schatz, M.F. Jarrold, Structural information from ion mobility measurements: effects of the long-range potential, J. Phys. Chem. 100 (1996) 16082–16086.
- [14] C. Ieritano, J. Crouse, J.L. Campbell, W.S. Hopkins, A parallelized molecular collision cross section package with optimized accuracy and efficiency, Analyst 144 (2019) 1660–1670.
- [15] S.A. Ewing, M.T. Donor, J.W. Wilson, J.S. Prell, Collidoscope: An improved tool for computing collisional cross-sections with the trajectory method, J. Am. Soc. Mass. Spectrom. 28 (2017) 587–596.
- [16] C. Larriba, C.J. Hogan Jr., Free molecular collision cross section calculation methods for nanoparticles and complex ions with energy accommodation, J. Comput. Phys. 251 (2013) 344–363.
- [17] C. Larriba, C.J. Hogan Jr., Ion mobilities in diatomic gases: measurement versus prediction with non-specular scattering models, J. Phys. Chem. 117 (2013) 3887–3901.
- [18] C. Larriba-Andaluz, F. Carbone, The size-mobility relationship of ions, aerosols, and other charged particle matter, J. Aerosol Sci. (2020), 105659.
- [19] G.H. Wannier, Motion of gaseous ions in a strong electric field. II, Phys. Rev. 87 (1952) 795.
- [20] V. Shrivastav, M. Nahin, C.J. Hogan, C. Larriba-Andaluz, Benchmark comparison for a multi-processing ion mobility calculator in the free molecular regime, J. Am. Soc. Mass Spectrom. (2017) 1–12.
- [21] J. Coots, V. Gandhi, T. Onakoya, X. Chen, C. Larriba-Andaluz, A parallelized tool to calculate the electrical mobility of charged aerosol nanoparticles and ions in the gas phase, J. Aerosol Sci. (2020), 105570.
- [22] V.D. Gandhi, C. Larriba-Andaluz, Predicting ion mobility as a function of the electric field for small ions in light gases, Anal. Chim. Acta (2021), 339019.
- [24] S. Lin, L. Viehland, E. Mason, Three-temperature theory of gaseous ion transport, Chem. Phys. 37 (1979) 411–424.
- [25] L.A. Viehland, S. Lin, Application of the three-temperature theory of gaseous ion transport, Chem. Phys. 43 (1979) 135—144.
- [26] L.A. Viehland, D.E. Goeringer, Moment theory of ion motion in traps and similar devices: I. General theories, J. Phys. B Atom. Mol. Opt. Phys. 38 (2005)

- 3987.
- [27] L.A. Viehland, Velocity distribution functions and transport coefficients of atomic ions in atomic gases by a Gram—Charlier approach, Chem. Phys. 179 (1994) 71–92.
- [28] H. Skullerud, On the calculation of ion swarm properties by velocity moment methods, J. Phys. B Atom. Mol. Phys. 17 (1984) 913.
- [29] P. Patterson, Temperature dependence of helium-ion mobilities, Phys. Rev. 2 (1970) 1154.
- [30] L.A. Viehland, C.-L. Yang, Improved techniques for the calculation of ab initio ion-neutral interaction potentials: application to coinage metal ions interacting with rare gas atoms, Mol. Phys. 113 (2015) 3874—3882.
- [31] I. Campuzano, M.F. Bush, C.V. Robinson, C. Beaumont, K. Richardson, H. Kim, H.I. Kim, Structural characterization of drug-like compounds by ion mobility mass spectrometry: comparison of theoretical and experimentally derived nitrogen collision cross sections, Anal. Chem. 84 (2012) 1026–1033.
- [32] H. Kim, H.I. Kim, P.V. Johnson, L.W. Beegle, J. Beauchamp, W.A. Goddard, I. Kanik, Experimental and theoretical investigation into the correlation between mass and ion mobility for choline and other ammonium cations in N2, Anal. Chem. 80 (2008) 1928–1936.
- [33] M.F. McGuirk, L.A. Viehland, E.P. Lee, W. Breckenridge, C.D. Withers, A.M. Gardner, R.J. Plowright, T.G. Wright, Theoretical study of Ba n+-RG (RG=rare gas) complexes and transport of Ba n+ through RG (n=1, 2; RG=He-Rn), J. Chem. Phys. 130 (2009), 194305.
 [34] A.A. Buchachenko, L.A. Viehland, Interaction potentials and transport prop-
- [34] A.A. Buchachenko, L.A. Viehland, Interaction potentials and transport properties of Ba, Ba+, and Ba2+ in rare gases from He to Xe, J. Chem. Phys. 148 (2018) 154304
- [35] L.A. Viehland, J.J. Hurly, Absence of quantum-mechanical effects on the mobility of argon ions in helium gas at 4.35 K, J. Chem. Phys. 105 (1996) 11143–11146.
- [36] P. Pathak, M.A. Baird, A.A. Shvartsburg, Identification of isomers by multidimensional isotopic shifts in high-field ion mobility spectra, Anal. Chem. 90 (2018) 9410—9417.
- [37] P. Pathak, M.A. Baird, A.A. Shvartsburg, Structurally informative isotopic shifts in ion mobility spectra for heavier species, J. Am. Soc. Mass Spectrom. 31 (2019) 137–145.
- [38] R. Wojcik, G. Nagy, I.K. Attah, I.K. Webb, S.V. Garimella, K.K. Weitz, A. Hollerbach, M.E. Monroe, M.R. Ligare, F.F. Nielson, SLIM ultrahigh resolution ion mobility spectrometry separations of isotopologues and isotopomers reveal mobility shifts due to mass distribution changes, Anal. Chem. 91 (2019) 11952—11962.
- [39] C.P. Harrilal, V.D. Gandhi, G. Nagy, X. Chen, M.G. Buchanan, R. Wojcika, C.R. Conant, M.T. Donor, Y.M. Ibrahim, S.V.B. Garimella, R.D. Smith, C. Larriba-Andaluz, Measurement and theory of gas phase ion mobility shifts Re-sulting from isotopomer mass distribution changes, Anal. Chem. (2021) (under review).



Carlos Larriba-Andaluz got his bachelor's degree in Aerospace at the Universidad Politecnica de Madrid. He moved to the States after an abridged stay at Iberia Airlines. He got his Ph.D. in Mechanical Engineering from Yale University in 2010 followed by a postdoctoral Associate and Ramon Areces Fellow at the University of Minnesota in the department of Mechanical Engineering. In 2015 he started a tenure-track position at the Purdue University School of Engineering and Technology in Indianapolis. His main area of research is steered towards Ion Mobility Spectrometry (IMS) coupled with Mass Spectrometry (MS).